THE VISCOELASTIC BEHAVIOUR OF COALS DURING PYROLYSIS

John W Patrick, Karen M Steel, Miguel Castro Diaz, ,
Colin E Snape
Nottingham Fuel and Energy Centre, SChEME, University of Nottingham, Nottingham, NG7 2RD, UK.
Corresponding author e-mail address: john.patrick@nottingham.ac.uk

Introduction

In the process of forming metallurgical coke, coal is heated in the absence of oxygen to cause both phase changes and chemical reactions to take place that lead to the release of volatile compounds and the 'softening' of the coal to form a fluid phase. The temperature at which softening starts depends on coal rank, particle size and heating rate, and is usually around 350°C. Upon further heating, the viscosity of the fluid phase decreases to a minimum and the rate of volatile release reaches a maximum. As temperatures increase still further, the viscosity increases as the softened mass resolidifies, leading to the final coke product. The coking of certain coals can cause excessive pressure to be exerted on the oven walls which is damaging. The reasons why certain coals give rise to high coking pressures are still largely unknown and there are no simple and precise tests for predicting coking pressure for a given coal.

As shown in Loison [1], graphs of coking pressure plotted against time generally show two peaks which vary significantly in size between different coals. The first peak occurs early on in the process and is usually broad, while the second peak is sharper and occurs toward the end of the process. These peaks are thought to be due to two different events occurring at different stages of the coking process. In the first stage, the temperature at the coal charge centre is <350°C and there are two plastic layers surrounding unfused coal. It is thought that pressure on the walls during this phase may be due to swelling of the plastic zone, and connected to the equilibrium between swelling of the plastic zone and contraction of the semicoke. In the second stage the temperature at the coal charge centre is >350°C. In this stage, the two plastic layers meet and there is a sharp increase in pressure on the walls. It is thought that the pressure may be caused by gases becoming trapped in the diminishing coal region, accumulating, and finally forcing their way out abruptly. The likelihood of this is strongly thought to be connected to the viscosity of the fluid phase.

The fluid phase has been measured using a Gieseler plastometer [2] which, for the last 60 years, has provided valuable empirical measurements of fluidity. However, these measurements have not provided a useful model with which to predict coking pressure. Rheometry and ^{1}H nuclear magnetic resonance (NMR) spectroscopy are brought together in this paper to study the fluid phase and elucidate possible mechanisms for coking pressure from which a model might be developed for predicting coking pressure for a given coal.

Nomura [3] showed that small amplitude oscillatory shear rheometry could be used to measure the viscoelastic properties of coal. The complex viscosity (η*) was determined, which is given by Eq. 1.

$$|\eta^*| = \frac{\sqrt{(G')^2 + (G'')^2}}{\omega} \quad (1)$$

where: ω = frequency.

G' = storage modulus (proportional to the energy which is stored and recovered).

G'' = loss modulus (proportional to the energy dissipated in flow).

Studies on a range of coals showed that as softening began at around 400°C, η* decreased to a minimum value before increasing at higher temperatures. Complex viscosities of the coals studied were found to lie in the range of 1×10^4 - 6×10^5 Pa.s, using a strain (γ) of 0.1% and a ω of 6.28 rad/s. Variation in ω showed that the fluid phase was shear thinning. Therefore, it was suggested that the Gieseler plastometer may underestimate the minimum viscosity due to structural changes incurred by the higher shear rates. Further work by Yoshida [4] on ten coals compared results obtained from the rheometer and the Gieseler plastometer and found that the temperatures at which changes occur were in fairly good agreement.

The second technique used to measure fluidity during pyrolysis is high temperature ^{1}H nuclear magnetic resonance (NMR) spectroscopy. This technique determines the fluidity evolving in a sample through the analysis of spectra acquired at different temperatures. The spectra are usually deconvoluted into two components, namely a Lorentzian distribution function that originates from the protons associated to the mobile phase in the sample, and a Gaussian distribution function that originates from the protons associated to the rigid phase. Further, the spin-spin relaxation time (T_2) is inversely proportional to the peak width at half height ($\Delta H_{½}$) as indicated by Eq. 2 and gives information about the mobility of the phase.

$$T_2 = \frac{1}{\pi \Delta H_{½}} \quad (2)$$

Although this straightforward relationship is only fulfilled for Lorentzian distribution functions, it is generally used to determine the mobility of both fluid and rigid phases. An increase in temperature causes an increase in the mobility of the phase, and therefore, a decrease in $\Delta H_{½}$ and an increase in T_2.

This technique has been used to determine the concentration and mobility of the fluid and rigid phases in coals [5], to characterise the extent of fusion or interaction between components of a blend during carbonisation [6] and to elucidate the effect of macerals on fluidity development [7]. In a more detailed work [8], it was found that Australian coking coal blends undergo significant positive and negative interactions, which increase with increasing difference in rank and fluidity between the coals. Moreover, these interactions were directly related to the fluid material evolving from inertinite and vitrinite.

Experimental

A range of coal samples with varying coking behaviours were tested. Table 1 shows properties of the samples, including Gieseler and coking pressure data. B1, B2 and B3 are blends with compositions given in Table 2. The samples contain an increasing concentration of C7 coal from B1 to B3.

Coking tests for the determination of wall pressure were carried out in a 250 kg moveable wall oven and tests for the determination of internal gas pressure were carried out in a 25 kg oven.

Table 1: Properties of Coal Samples.

	volatile matter daf (wt%)	swelling index	Gieseler T_s (°C)	Gieseler T_{mf} (°C)	Gieseler T_r (°C)	max. fluidity (ddpm)	wall pressure 250 kg oven (kPa)
C1	32.8	6.75	387	448	489	29783	3
C2	19.3	8.00	439	473	500	37	15.9
C3	17.9	7.75	440	479	507	37	48.4
C4	32.1	5.50	381	443	486	26810	2
C5	25.3	6.75	400	452	487	1726	2.4
C6	26.1	8.00	396	454	493	2954	3.7
B1	19.5	-	418	457	487	94	4.1*
B2	18	-	436	466	487	16	5.8*
B3	17.1	-	442	460	486	6	12.9*
C5	25.3	6.75	400	452	487	1726	1.2*
C6	26.1	8.00	396	454	493	2954	7.1*

* - 25 kg oven, internal gas pressure (not wall pressure).

T_s, T_{mf}, T_r - temperature for softening, maximum fluidity and re-solidification respectively.

Table 2: Composition of B1, B2 and B3 coal blends.

Coal Blend	C7 (%)	Amonate (%)	Marfork (%)	Coke dust (%)	Ash (%)
B1	**40**	40	10	10	17.1
B2	**50**	40	0	10	6.8
B3	**70**	20	0	10	5.8

Rheological measurements were performed using a Rheometrics RDA-III high-torque controlled strain rheometer. Coal samples (<50 μm) were pressed under 5 tonnes of pressure in a 25 mm die to form discs with a thickness of approximately 2.6 mm. The test involved placing the disc of coal between two 25 mm parallel plates, which had serrated surfaces to reduce 'slippage'. The sample was heated quickly to 330°C and then heated to 600°C at a rate of 3°C/min. A constant flow of N_2 was used to transfer heat to the sample and remove volatiles. Tests were performed with a strain of amplitude 0.1% and a frequency of 1 Hz (6.28 rad/s). This was applied to the sample throughout the heating period. The stress response was measured to obtain linear viscoelastic properties as a function of temperature. Throughout the test, a constant normal force of 200 g was applied to the sample to reduce slippage. Therefore, the thickness of the sample was allowed to change.

The thickness could be measured throughout the test and gives an indication of how much the sample is expanding.

A Doty 200 MHz ^{1}H NMR probe was used with a Bruker MSL300 instrument for the NMR fluidity development studies. Again, a constant flow of N_2 was used to transfer heat to the samples and to remove the volatiles. The solid echo pulse sequence (90° - τ - 90°) was used to determine the variation in peak width as a function of temperature. The pulse length was increased from 3.5 μs at room temperature to 4.85 μs at the final temperature. Approximately 140-150 mg of sample was packed lightly into a boron-nitride container and 200 scans were accumulated using a recycle delay of 0.3 s. The samples were heated at a rate of 5°C/min from room temperature to approximately 320°C by increments of 25°C, and then by increments of 10°C to the final temperature. Correspondingly, lag times of 3.45 and 1.50 minutes were introduced before data acquisition to stabilise the temperature reading from the probe thermocouple.

Results

Rheometry

Figure 1 shows the complex viscosity (η*) of C1, C2 and C3 coals as a function of temperature. There is little change in the samples at temperatures up to 400°C. For C1 coal, η* begins to decrease at 400°C, indicating that the sample is softening and becoming less elastic. At 428°C, there is a dramatic change and the sample becomes considerably less elastic. The material behaves more like a fluid and η* reaches a minimum value of 2.92×10^4 Pa.s at 446°C. As the temperature increases above 446°C, elasticity increases and the sample begins to resolidify with resolidification almost complete at 480°C. For C2 coal, η* begins to increase at 400°C to a peak at 450°C. It is thought that at temperatures less than 400°C, the particles are slipping past each other under the strain and that as the temperature increases above 400°C, the particles begin to soften and lock together more firmly, causing η* to increase. Therefore, the measurements for C2 below 450°C are not considered to reflect the viscoelastic properties of the sample. As the temperature increases above 450°C, softening becomes far more pronounced and η* begins to decrease, decreasing markedly at 464°C to a minimum of 1.05×10^5 Pa.s at 465°C. Above 465°C the sample begins to re-solidify with re-solidification essentially complete by 510°C. Compared to C1 coal, C2 does not become as fluid and reaches its minimum η* of approximately 10^5 Pa.s at a higher temperature. No distinct fluid phase was detected for C3 coal at temperatures up to 500°C. Interestingly, η* begins to decrease at 500°C, decreasing to 1.1×10^5 Pa.s at 600°C.

Figure 2 shows η* for three coal blends, which have an increasing concentration of C7 coal from B1 to B3 (compositions shown in Table 2). All samples began to soften slightly at 440°C and more considerably at 460°C, 465°C and 480°C for B1, B2 and B3 respectively. The complex viscosities decrease to similar minimum values of approximately 2×10^5 Pa.s. However, this occurs at different temperatures of 467°C, 471°C and 485°C for B1, B2 and B3 respectively. The temperature range at which the samples are fluid decreases substantially from B1 to B3. It is interesting that there appears to be a significant second region of softening at temperatures greater than 500°C for B3, which is very similar to that observed for C3 coal.

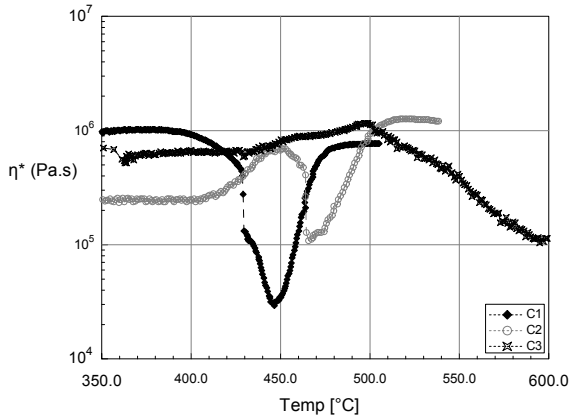

Figure 1: Complex viscosity of C1, C2 and C3 coals as a function of temperature (γ = 0.1%, ω = 6.28 rad/s).

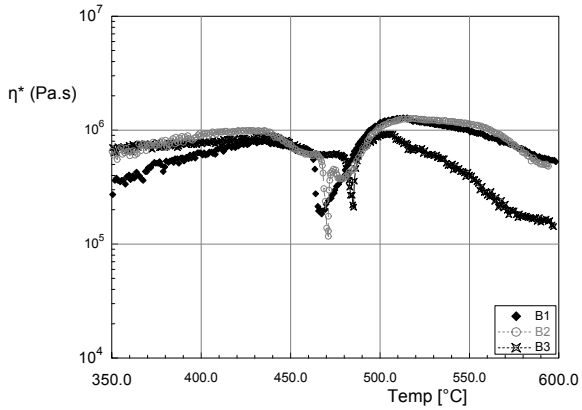

Figure 2: Complex viscosity of B1, B2 and B3 coal blends as a function of temperature (γ = 0.1%, ω = 6.28 rad/s).

Figure 3 shows η* for C4, C5 and C6 coals. The complex viscosity curve for C4 is very similar to C1, shown in Fig. 1, with a minimum η* of 1.26 $\times 10^4$ Pa.s. C5 shows a similar behaviour to C2 and B1, with η* decreasing to only 1.03 $\times 10^5$ Pa.s, yet this minimum η* occurs at a lower temperature of 450°C. C6 was found to be the most fluid coal measured with η* decreasing to 1 $\times 10^4$ Pa.s at 455°C and the fluid region persisting over a wide temperature range.

^{1}H NMR spectroscopy

Figure 4 shows the peak width at half height ($\Delta H_{1/2}$) of the proton NMR spectra for C1, C2 and C3 coals as a function of pyrolysis temperature. The temperature of maximum fluidity (T_{mf}) increases from C1 to C2 and to C3, and the magnitude of the fluidity increases in the reverse order. The $\Delta H_{1/2}$ of the proton NMR spectra for the coal blends B1, B2 and B3 are shown in Fig. 5. The T_{mf} increases from B1 to B3 and the magnitude of the fluidity increases in the reverse order. Fig. 6 shows $\Delta H_{1/2}$ of the proton NMR spectra of C4, C5 and C6. C4 shows a very similar trend to C1. The T_{mf} for C5 is less than that for the blends and C2 and C3 coals yet higher than that for C1 and C4 coals. C6 shows a very similar trend to C5 coal.

From the NMR spectra for all coal samples, Table 3 shows the percentage of the spectra which follows Gaussian and Lorentzian distributions at the temperatures of maximum fluidity, and their T_2 values. C4, C6 and C1 coals contain the most amount of fluid material, with more than 60% of the hydrogen becoming mobile. The fluid phase of C1 coal has the highest mobility followed by C4. C5 contains the next highest concentration of fluid material with a mobility less than C1 and C4 coals yet similar to C6. The next highest concentrations of fluid material are found in B1, B2, C2 and B3 samples, and of these samples, the fluid phase of C2 shows the highest mobility, followed by B1, B2 and B3. C3 coal has the least amount of fluid material, which has the least mobility.

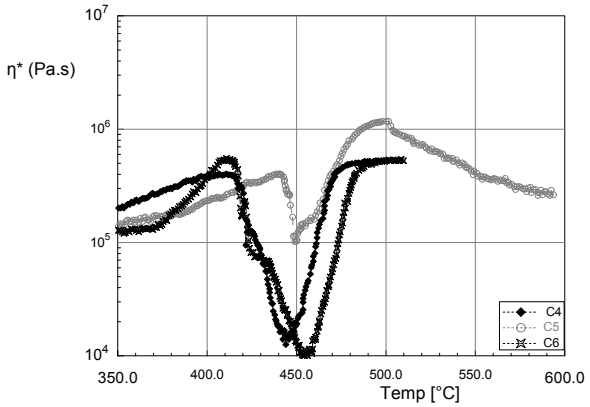

Figure 3: Complex viscosity of C4, C5 and C6 coals as a function of temperature (γ = 0.1%, ω = 6.28 rad/s).

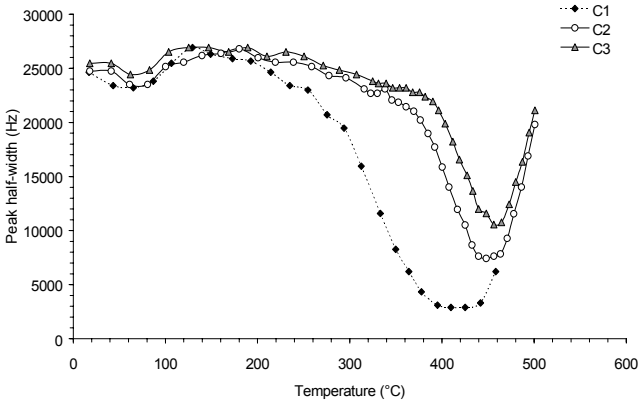

Figure 4: Peak half-width ($\Delta H_{1/2}$) of ^{1}H NMR spectra for C1, C2 and C3 coals as a function of temperature.

Table 3: Percentage of ^{1}H NMR spectra following Gaussian (G) and Lorentzian (L) distributions at T_{mf} (based on area), and T_2 values from spectra and G and L distributions.

	^{1}H NMR spectra (%)		T_2 (µs)		
	G	**L**	**overall**	**G**	**L**
C4	14	86	96	44	100
C6	31	69	77	25	90
C1	38	62	110	21	121
C5	51	49	70	19	91
B1	59	41	45	17	70
B2	62	38	39	17	63
C2	64	36	43	18	74
B3	65	35	32	16	59
C3	68	32	30	18	58

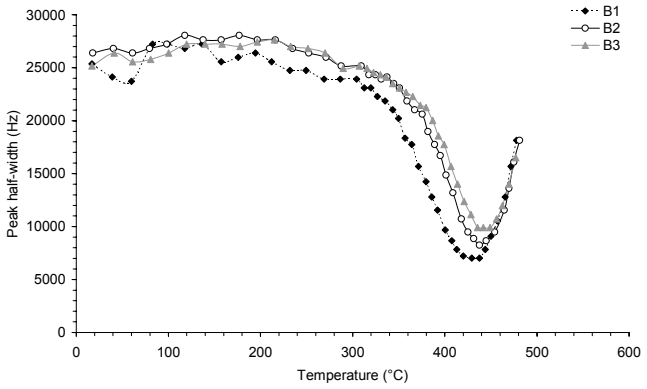

Figure 5: Peak half-width ($\Delta H_{1/2}$) of ^{1}H NMR spectra for B1, B2 and B3 coal blends as a function of temperature.

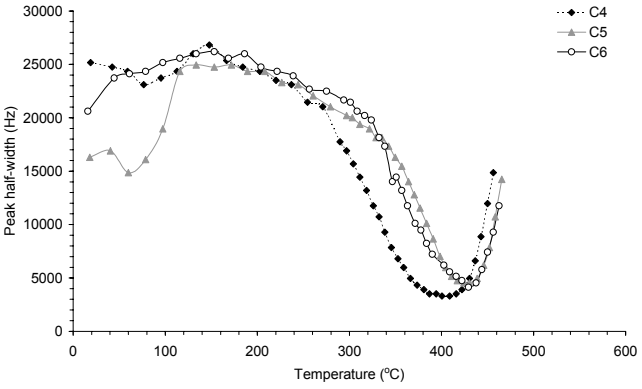

Figure 6: Peak half-width ($\Delta H_{1/2}$) of ^{1}H NMR spectra for C4, C5 and C6 coals as a function of temperature.

Discussion

The rheometer and NMR results for C1, C2 and C3 coals compare well and also compare well with results obtained from the Gieseler plastometer. Both the temperatures at which changes occur and the magnitude of fluidity are fairly consistent. However, the Gieseler plastometer measured the same maximum fluidity of 37 ddpm for both C2 and C3 coals, which is not consistent with the rheometer and NMR results, and the rheometer did not detect a distinct fluid phase at temperatures less than 500°C for C3 coal, which is not consistent with the Gieseler and NMR results. However, it may be possible to detect a fluid phase by using a lower frequency than 6.28 rad/s.

C1, C2 and C3 coals generated wall pressures of 3, 15.9 and 48.4 kPa, respectively. Based on the rheometer and NMR results, it appears that high wall pressures occur when only a small amount of fluid material forms, and when this fluid material has a low fluidity. It is thought that the coal particles fuse together and, due to the highly viscous nature of the mass, volatiles are unable to permeate through. The free movement of gas may be critical for the release of gas and the prevention of gas pressure build up. This may be achieved by creating a pore and fissure network through which the gas can pass. Perhaps, without this free movement the gas is forced to the coal side where it builds up in a diminishing region until the final coal particles fuse. At this point the gas is forced to escape, causing an abrupt increase in pressure on the walls.

The rheometer, NMR and Gieseler results also compare fairly well for B1, B2 and B3 blends. The internal gas pressures measured during coking for these samples were 4.1, 5.8 and 12.9 kPa, respectively. The results greatly assist the proposal made above that high gas pressures may occur when both the amount of fluid material generated and the mobility of that material are both low. In addition, the magnitude of pressure generated may be directly related to the T_{mf}, such that the higher the T_{mf}, the higher the gas pressure generated.

The rheometer, NMR and Gieseler results for C4 coal compare well and are very similar to the results obtained for C1 coal. Both C4 and C1 coals formed large amounts of fluid material (>60%) which had high mobilities, and both generated low coking pressures of only 2 and 3 kPa, respectively. C5 also generated a low coking pressure of only 2.4 kPa, but the concentration of mobile hydrogen was considerably less at approximately 50%. By comparison, the concentration of mobile hydrogen for C2, which generated a significant coking pressure, was 36%. It may be that there is a threshold for mobile hydrogen, below which coking pressure is generated. This builds onto the mechanism proposed above. Perhaps when the amount of mobile hydrogen is below a threshold which lies somewhere in the region of 35-45%, the pockets of fluid material which form do not link up to form passages for gas to flow through the rigid network and out to the coke side. The gas is forced to the coal side, where it builds up. The mobility of the fluid phase may also play a part in restricting gas flow.

C6 coal generated a wall pressure of 3.7 kPa, which is slightly higher than the wall pressures generated for C1 and C4 coals. In addition, the internal gas pressure was also found to be significant. The reason for this pressure is thought to be purely due to the coal charge expanding as it converts to gas and liquid phases. During some

rheometer tests, the thickness of the sample was monitored. When only a minimal normal force was applied, C1, C4 and C6 coals expanded the most, with C6 expanding by almost 180% while C4 and C1 expanded by approximately 120%.

This work suggests that there may be two mutually exclusive mechanisms behind the generation of coking pressure, where the two extreme possible states for the fluid phase can lead to pressure on oven walls. This agrees with previous assessments, where the coking pressure curves suggest two mutually exclusive mechanisms (Loison et al. (1989)). Further tests on more coal samples need to be performed to confirm this hypothesis. The reason why a model correlating Gieseler fluidity with coking pressure has not been established may be due to the problem coals being at either end of the fluidity spectrum. The Gieseler plastometer has been designed to be able to obtain empirical measurements of the fluid phase over a broad range of possible fluidities, but it may not cover the full range. The Gieseler gave similar fluidity values for C2 and C3 coals and yet these two coals behave very differently in the rheometer and NMR instruments and generate different coking pressures. At the other end, the Gieseler recorded only 2954 ddpm for C6 coal yet this coal was found to be by far the most fluid coal measured using the rheometer.

Conclusion

It is proposed that coking pressure may occur through two mutually exclusive mechanisms, with each case occurring when the fluidity is at either end of the fluidity spectrum. Coking pressure was found to occur for low volatile matter coals which formed only a small amount of fluid material (< ~40%) and for which the overall mobility was low (T_2 < ~40 μs). In this case it is proposed that the fused coal forms a rigid network containing pockets of fluid material which are largely unconnected and therefore present an impermeable barrier for gas flow, trapping the gas in the centre of the coal charge where it builds up and eventually causes pressure to be exerted on the walls. The magnitude of the pressure generated for this mechanism may be inversely proportional to both the percentage of mobile hydrogen and the mobility of the fluid phase, and proportional to the temperature of maximum fluidity. Coking pressure was also found to occur for a high volatile matter coal which formed a highly fluid phase over a broad temperature range. In this case it is proposed that the expansion of the coal charge as it produces gas and liquid phases causes pressure to be exerted on the walls. The rheometer and NMR instruments used in this work have provided very precise characterisations of fluidity development at the microstructure level and could enable improved models to be developed for predicting coking pressure and coke quality.

Acknowledgements

The authors thank the ECSC for funding the work at the Nottingham Fuel and Energy Centre. The contributions of INCAR-CSIC, Oviedo, Spain and CPM, France in providing respectively the wall pressure and internal gas pressure data, are also gratefully acknowledged.

References

1. Loison R., Foch P. and Boyer A. (1989). Coke - Quality and Production, Butterworths, p 369.

2. Standard Test Method for Plastic Properties of Coal by the Constant-Torque Gieseler Plastometer. (1997). American Standard for Testing Materials (ASTM) Designation: D 2639-97
3. Nomura S., Kato K., Komaki I., Fujioka Y., Saito K. and Yamaoka I. (1999). Viscoelastic properties of coal in the thermoplastic phase, Fuel, 78, 1583-1589
4. Yoshida T., Iino M., Takanohashi T. and Katoh K. (2000). Study of thermoplasticity of coals by dynamic viscoelastic measurement: effect of coal rank and comparison with Gieseler fluidity, Fuel, 79, 399-404
5. Snape C.E., Martin S.C. (2000). Quantifying fluidity development and mobility in coals by in situ ^{1}H NMR, Prepr. Symp. Am. Chem. Soc. Div. Fuel Chem., 45 (2), 205-210.
6. Sakurovs R. and Lynch L.J. (1993). Direct observations on the interaction of coals with pitches and organic compounds during co-pyrolysis, Fuel, 72, 743-749.
7. Maroto-Valer M.M., Taulbee D.N., Andrésen J.M., Hower J.C. and Snape C.E. (1998). The role of semifusinite in plasticity development for a coking coal, Energy & Fuels, 12, 1040-1046.
8. Sakurovs R. (2003). Interactions between coking coals in blends, Fuel, 82, 439-450.